Review Article

Myocardial blood flow quantification for evaluation of coronary artery disease by computed tomography

Filippo Cademartiri[1,2], Sara Seitun[3], Alberto Clemente[4], Ludovico La Grutta[5], Patrizia Toia[5], Giuseppe Runza[6], Massimo Midiri[5], Erica Maffei[1]

[1]Department of Radiology, Montreal Heart Institute, Université de Montreal, Montreal, Canada; [2]Department of Radiology, Erasmus Medical Center University, Rotterdam, The Netherlands; [3]Department of Radiology, IRCCS AOU San Martino-IST, Genoa, Italy; [4]Department of Radiology, Fondazione Toscana Gabriele Monasterio, Pisa and Massa, Italy; [5]Department of Radiology, University of Palermo, Palermo, Italy; [6]Department of Radiology, P.O. Umberto I, Azienda Sanitaria Provinciale 8, Siracusa, Italy

Contributions: (I) Conception and design: F Cademartiri, S Seitun, E Maffei; (II) Administrative support: F Cademartiri, S Seitun, E Maffei; (III) Provision of study materials or patients: F Cademartiri, S Seitun, E Maffei, A Clemente; (IV) Collection and assembly of data: All authors; (V) Data analysis and interpretation: All authors; (VI) Manuscript writing: All authors; (VII) Final approval of manuscript: All authors.

Correspondence to: Prof. Dr. Filippo Cademartiri, MD, PhD, FESC, FSCCT. Department of Radiology, Montreal Heart Institute, Centre de Recherche, room S-2530, 5000 Rue Belanger, Montreal, QC - H1T 1C8, Canada. Email: filippocademartiri@gmail.com.

Abstract: During the last decade coronary computed tomography angiography (CTA) has become the preeminent noninvasive imaging modality to detect coronary artery disease (CAD) with high accuracy. However, CTA has a limited value in assessing the hemodynamic significance of a given stenosis due to a modest specificity and positive predictive value. In recent years, different CT techniques for detecting myocardial ischemia have emerged, such as CT-derived fractional flow reserve (FFR-CT), transluminal attenuation gradient (TAG), and myocardial CT perfusion (CTP) imaging. Myocardial CTP imaging can be performed with a single static scan during first pass of the contrast agent, with monoenergetic or dual-energy acquisition, or as a dynamic, time-resolved scan during stress by using coronary vasodilator agents (adenosine, dipyridamole, or regadenoson). A number of CTP techniques are available, which can assess myocardial perfusion in both a qualitative, semi-quantitative or quantitative manner. Once used primarily as research tools, these modalities are increasingly being used in routine clinical practice. All these techniques offer the substantial advantage of combining anatomical and functional evaluation of flow-limiting coronary stenosis in the same examination that would be beneficial for clinical decision-making. This review focuses on the state-of the-art and future trends of these evolving imaging modalities in the field of cardiology for the physiologic assessments of CAD.

Keywords: Cardiac computed tomography; coronary artery disease (CAD); stress imaging; myocardial perfusion imaging; myocardial blood flow quantification

Submitted Jan 05, 2017. Accepted for publication Mar 15, 2017.
doi: 10.21037/cdt.2017.03.22
View this article at: http://dx.doi.org/10.21037/cdt.2017.03.22

Introduction

Since its introduction more than 15 years ago, coronary computed tomography angiography (CTA) has become the preeminent noninvasive imaging modality to detect coronary artery disease (CAD) in patients with low-to-intermediate probability of CAD (1-3). Importantly, CTA detects significant (≥50% lumen reduction) CAD with high accuracy offering excellent sensitivity and negative predictive value (NPV) (≥95%) for the diagnosis of CAD (4).

Furthermore, the long-term prognostic value of CTA for adverse cardiovascular events in subjects with suspected or known CAD have been reported, showing excellent long-term prognosis when there is no evidence of atherosclerosis

and allowing risk stratification according to the presence, extent, and severity of CAD (5,6).

Although CTA accurately assesses coronary plaque burden and stenosis, as well as ventricular function, it is limited in evaluating the hemodynamic significance of CAD due to the lack of functional information for a given stenosis.

This is an important limitation in light of the growing evidence of the benefit of the approach based on the evaluation of ischemia over the visual assessment of coronary stenosis in the management of patients with stable angina. In fact, several landmark studies such as the FAME and FAME-2 trials have demonstrated that a percutaneous coronary intervention (PCI) strategy guided by the invasive hemodynamic parameter, fractional flow reserve (FFR), may be superior to a strategy guided by invasive coronary angiography (ICA) alone, and thus revascularization should be guided by functional assessments of myocardial ischemia (7,8). Furthermore, a large randomized controlled trial, the COURAGE trial, have demonstrated that PCI based solely on standard visual approach offers no benefits over optimal medical therapy in reducing mortality, myocardial infarction, or other major cardiovascular events (9).

Without functional data, ICA and coronary CTA can only provide limited correlation with the evidence of myocardial ischemia (10). Therefore, CTA information should be routinely integrated with functional imaging data, such as single photon emission computed tomography (SPECT), stress echocardiography or stress perfusion magnetic resonance imaging (MRI), to guide coronary revascularization.

However, the new and rapid technical advantages of the multidetector row (≥64 slices) CT systems allow a robust imaging of the coronary arteries and a reliable assessment of myocardial CT perfusion (CTP) in the same examination.

First attempts of CTP at rest were conducted in the late 70' by using first-generation single section CT scanner (11,12). However, the advent of multidetector row (≥64 slices) CT systems, with improvement in temporal, spatial and contrast resolution as well as volume coverage due to increased detector rows, faster gantry rotation and smaller isotropic voxel size, allow CT to demonstrate myocardial perfusion at rest and during pharmacologic stress. Since 2005 with the first human report of CTP under adenosine stress condition by Kurata *et al.* (13), several clinical studies, including recent multicenter trials, have established the value of myocardial CTP compared to reference standards as SPECT, ICA (with or without FFR) and stress perfusion MRI (14-16).

Therefore, CTP imaging has emerged from mere research application to its clinical use in the identification of myocardial ischemia during stress by using coronary vasodilator agents (adenosine, dipyridamole, or regadenoson), combining in the same examination both functional and anatomical information (16). Furthermore, a CT-derived FFR measurement computed from resting coronary CTA images (FFR-CT) that applies computational fluid dynamics and the transluminal attenuation gradient (TAG), an intracoronary attenuation-based analysis of coronary CTA, have been recently introduced (17,18). These techniques allow for assessment of epicardial lesion-specific ischemia without the need of coronary vasodilation. The identification of a hemodynamic significant stenosis corresponds to a reduction in false positives identified by coronary CTA that can be used as a sensitive and safe gate-keeper for ICA (17,18).

Based on the technical aspects of different CT-based functional imaging techniques and clinical applications, the current review describes the state-of-the art of the technology with its advantages and disadvantages, and tries to anticipate future developments.

CTP imaging protocols

After intravenous injection of iodinated contrast agent (typically via the antecubital vein), CTP imaging analyzes the distribution of contrast material during its first-pass through the myocardium as a surrogate marker of myocardial blood flow (MBF), similarly to stress perfusion MRI. Because contrast enhancement increases proportionally with iodine concentration, hypo-attenuated/non-enhancing myocardial regions correlate with myocardial perfusion defects (19,20).

A comprehensive CT myocardial perfusion examination should include both rest and stress acquisitions in order to differentiate reversible from fixed myocardial perfusion defects (20). Narrow settings of window width and level and thick multiplanar reconstruction (MPR) of 5–8 mm slice thickness are recommended in order to detect subtle contrast difference between the hypo-perfused myocardium compared to normal myocardium (20).

A combined coronary CTA/CTP imaging protocol could be performed according to the rest/stress or stress/rest sequences, separated by 10–15 minutes to allow for contrast wash-out (*Figure 1*) (12,16).

In clinical practice the rest/stress protocol is the preferred approach for patients with low-to-intermediate probability of CAD, since it provides the advantage of the high NPV of the morphological coronary CTA acquisition to rule-

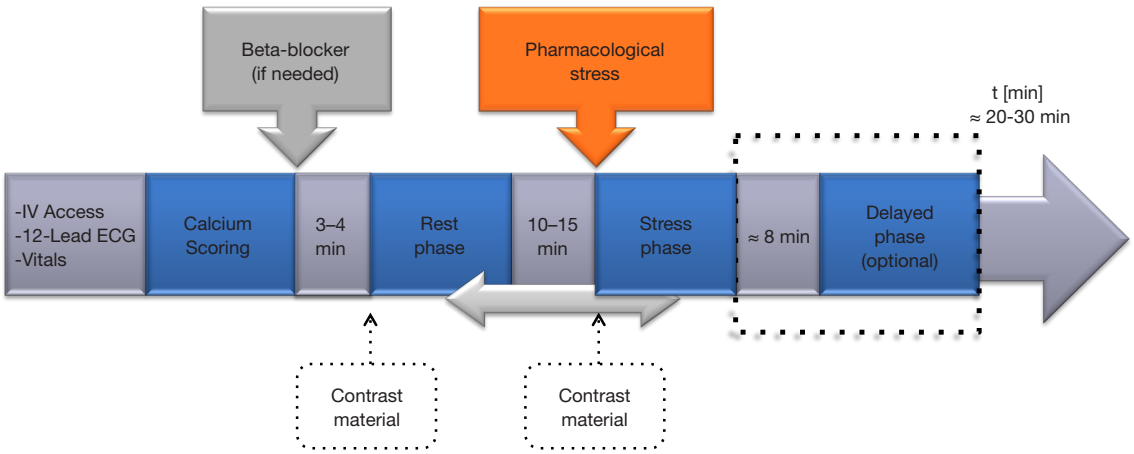

Figure 1 Flow-chart of a comprehensive CT perfusion imaging protocol that includes coronary artery calcium scoring, evaluation of coronary anatomy and perfusion at the rest phase, and assessment of myocardial perfusion during the stress phase. Delayed enhanced CT is optional. IV, intravenous.

out obstructive CAD. Indeed, stress CTP imaging could only be selectively performed in patients with intermediate or obstructive coronary stenosis to assess the physiological significance of CAD (16). This approach will obviate need for further testing with reductions in the radiation and contrast medium doses. This protocol is highly sensitive for the detection of necrosis, however, the risk of cross-contamination of contrast in the stress phase and the use of beta-blockers, may confound perfusion defects and decrease the sensitivity for myocardial ischemia (16).

Conversely, the stress/rest protocol could be more suitable for patients with high pre-test probability of CAD or patients with known CAD, in whom there is a high clinical suspicion of significant functional CAD (16). By reducing the risk of contrast media contamination, this protocol maximizes the sensitivity for the detection of ischemia. However, a fixed perfusion deficit may partially hyperenhance to differing degrees during the rest phase and this phenomenon should be considered while discriminating between viable and nonviable myocardium (20).

Furthermore, beta-blocker and nitrates may be administrated before the rest acquisition without interfering with the stress perfusion evaluation (16).

Rest phase

Generally, the rest acquisition is directly derived from the imaging dataset acquired for coronary anatomy (16).

The rest phase is less sensitive for the detection of myocardial ischemia, since resting blood flow through a diseased coronary artery is not decreased until the stenosis exceeds 85–90% of the luminal diameter because of coronary autoregulation (21,22). At this point resistive coronary arterioles (150–300 μm) can no longer dilate according to the autoregulation mechanism which maintains constant the coronary blood flow over range of perfusion pressures, and MBF starts decreasing (21,22).

Therefore, a subendocardial or transmural hypoenhancement in the rest phase may indicate a critical flow-limiting coronary artery stenosis or a myocardial necrosis/scar from infarction (*Figure 2*).

At the rest phase, other CT imaging signs of myocardial necrosis/fibrosis may be detected, such as (I) myocardial wall thinning; (II) lipomatous metaplasia (<10 HU); (III) myocardial calcifications; (IV) aneurysmal/pseudoaneurysmal dilation, and mural thrombus (20) (*Figure 2*). These data highlight the importance of rest imaging in myocardial perfusion evaluation (20).

Stress phase

In the ischemic cascade, stress perfusion abnormalities are more sensitive than wall motion abnormalities (16). After the seminal investigation from Gould *et al.* (21,22), it is well known that pharmacologically stimulated hyperemic MBF commonly decreases in the presence of a significant epicardial coronary artery stenosis exceeding 45% of luminal diameter. Therefore, compared to rest imaging, a

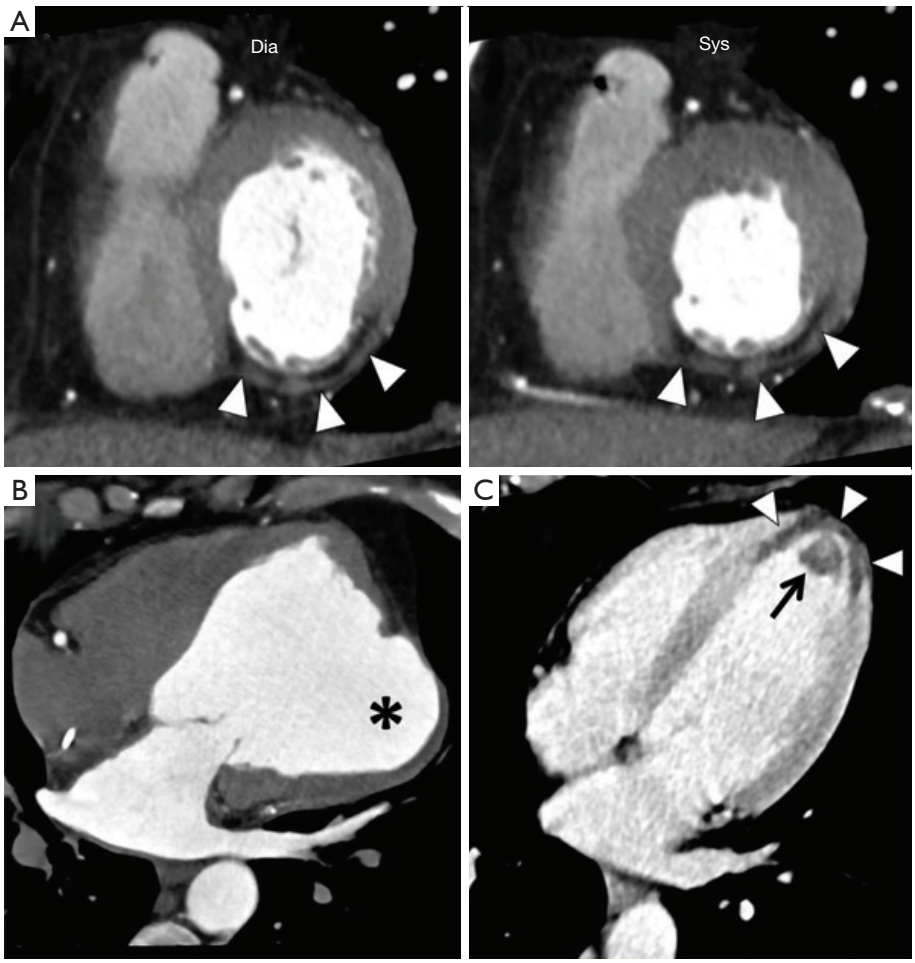

Figure 2 CT rest perfusion imaging of myocardial infarction. (A) Myocardial wall thinning associated with sub-endocardial hypoperfusion and adipose metaplasia are known signs of chronic infarction. Lipomatous metaplasia is usually seen as hypoattenuated areas (<0 HU) mostly in the subendocardial location (arrowheads). Concomitant akinesia is indicative of transmural infarction; (B) CT coronary angiography can depict with high spatial resolution ischemic morphological alterations of the myocardium, such as chronic post-ischemic aneurysmal dilation (asterisk in B); (C) in the setting of acute myocardial infarction, CT coronary angiography may demonstrate the severely hypoperfused myocardium with transmural extension in the apex and para-apical region (arrowheads) with associated apical thrombosis (arrow). Dia, diastole; Sys, systole.

vasodilator stress imaging is more likely to detect regions of myocardial ischemia (21). Vasodilators agents act through stimulation of A2 receptors in the microvasculature by both direct and endothelium-mediated mechanisms with a 3.5- to 4-fold increase in MBF (21). The most commonly used vasodilator stress agent in clinical practice for the purpose of myocardial CTP imaging is adenosine [140 μg/kg/min intravenously (IV) for 3 min] during ECG monitoring and continuous infusion, due to its short half-life in the seconds and rapid onset and short duration of action (16). However, dipyridamole (0.56–0.84 mg/kg body weight IV over 4–6 min) and regadenoson (0.4 mg IV bolus) have been used in clinical CTP studies (16). Dipyridamole has the advantage of lower cost, however, aminophylline may be administered after the stress agent to reverse its longer vasodilator effects (16). Regadenoson, a selective agonist of A2a receptor, has the advantages to reduce the side effects in patients with asthma or chronic obstructive pulmonary disease (16).

During the examination, vital parameters are monitored (heart rate with a 12-lead ECG as well as blood pressure and oxygen saturation).

Myocardial perfusion defects should be evaluated

according to the extent, severity (sub-endocardial or transmural), and location. A standardized 17-segment model of myocardial wall's segment according to the American Heart Association scientific statement for location of the perfusion defects is highly recommended (23). Integrating rest images with stress perfusion analysis identifies the degree of reversibility of a perfusion defect. The presence of reversible or partially reversible stress-induced subendocardial or transmural hypoattenuated area in the myocardium is consistent with myocardial ischemia (20). Conversely, a fixed perfusion defect, observed in both rest and stress phases, is indicative of myocardial necrosis/fibrosis (20). In some circumstances, a relative hyperenhancement of an infarct may be detected in the second scan acquisition if the imaging protocol stress-rest is employed (20).

Finally, the perfusion defects should be correlated with the anatomic localization of coronary stenosis on coronary CTA to match anatomy with the functional defects. The close correlation with CTA represents a crucial aspect for an accurate interpretation of CTP imaging, owing to the significant variability in normal coronary anatomy.

Late-enhancement phase

A delayed acquisition at 8–10 minutes may be also employed for the evaluation of myocardial viability. Nonviable myocardium will appear as a hyperdense area in the region of scar fibrosis (20). According to patient's BMI, use of low voltages such as 100, 90, 80 or even 70 kVp is preferable, since it results in higher CT attenuation than 120 kVp, because the X-ray output energy at these low voltages is closer to the iodine k edge of 33 keV, but at the expense of increased image noise (16).

However, late-enhancement scan is not routinely recommended in clinical practice due to the sub-optimal signal-to-noise and contrast-to-noise ratios of CT compared to late-enhancement MRI.

CTP imaging techniques

Myocardial flow/perfusion imaging and assessment

Two main techniques have been implemented for myocardial CTP imaging: static CTP imaging and dynamic CTP imaging.

For the static CTP, a single phase of the first-pass of contrast material through the myocardium is acquired with a monoenergetic or dual-energy method; whereas for the dynamic acquisition, a time-resolved scan allows to assess the wash-in and the wash-out kinetics of the contrast agent in the myocardium (16). By obtaining Time Attenuation Curve (TAC) computation, dynamic acquisition enables to calculate hemodynamic perfusion parameters from mathematical modeling (16).

Static CTP imaging—monoenergetic CT acquisition

The static CTP imaging during the arterial, first pass gives a snapshot of myocardial perfusion during a single stationary phase. It is of paramount importance the optimal timing for first-pass single-phase stress CTP to improve diagnostic accuracy. According to literature, studies of analysis of the TACs obtained from dynamic CTP acquisition under pharmacological stress using adenosine, revealed that the maximum attenuation difference between ischemic and non-ischemic myocardium occurred from 24–32 seconds (24) and 18–30 seconds (25) after initiation of contrast media injection or at 2–6 seconds from the time of maximal enhancement in the ascending aorta (26). However, other hemodynamic parameters such as cardiac output and flow rate of the contrast material may affect bolus timing (27). The flow rate of injected contrast medium should be high, at least 5 mL/s, to allow for high differences in contrast enhancement (24).

Besides the retrospective ECG-gating (with prospective tube current modulation) (28,29), the introduction of prospective ECG-gating (30,31) and prospectively ECG-triggered high-pitch spiral acquisition implemented with the second generation 128-slice dual-source CT (DSCT) scanner (32,33) allows for a reduction in contrast media volume and dose profile with approximately one order of magnitude, often to sub-millisievert dose levels (32).

The analysis of perfusion is qualitative by visual interpretation of the hypo-enhanced regions of the myocardium with respect to the normal remote myocardium, using a standard of normality learned with experience (16) (*Figure 3*).

Automated software providing modeling of the perfusion data into a 3D volume-rendering of the left ventricle, as well as into a 17-segment polar map, are readily available (*Figure 3*).

Finally, automated software application allows for evaluation of the transmural perfusion ratio (TPR, an endocardial-to-mean epicardial ratio of attenuation values) using a 17-segment bull's-eye plot. However, this semi-quantitative index parameter seems to be not reliable in the presence of prior infarction or significant beam-hardening

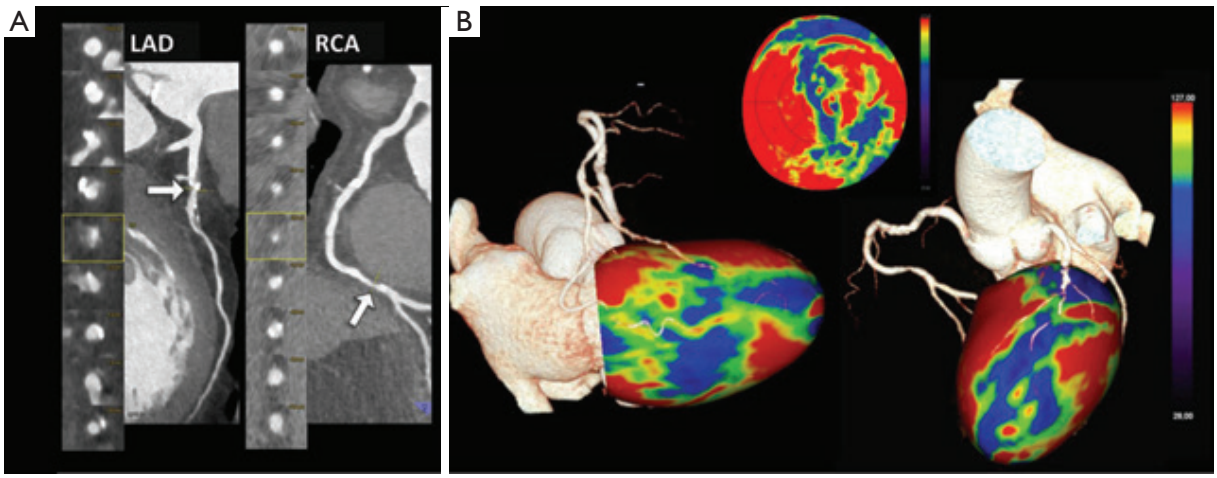

Figure 3 Static monoenergetic CT myocardial perfusion imaging. A 77-year-old male patient presented with atypical chest pain. (A) Coronary CT angiography showed a critical stenosis (>70% luminal narrowing) at the proximal segment of the left anterior descending artery (LAD) and at the distal segment of the right coronary artery (RCA) sustained by atherosclerotic plaques, arrows; (B) three-dimensional volume-rendering modeling of the left ventricular myocardial perfusion data with superimposed coronary tree, acquired with a prospectively ECG triggered high-pitch spiral technique at stress during the first pass, arterial phase, showed the presence of extensive perfusion defects at the inferior (left) and anterior (right) wall, color-coded in blue/green. Perfusion deficits are also presented in a 17-segment polar plot (top).

or motion artifacts (20).

Static CTP imaging—dual-energy CT acquisition

Dual-energy computed tomography (DECT) was first introduced in the late 1970s and allows for the differentiation of materials based on their X-ray attenuation at different tube voltages (34). The DECT technique allows the simultaneous acquisition of CT data using two different photon spectra (at 80/90/100 kV and 140/150 kV) of distinctly different mean energies within a single helical acquisition (34). With this technique pure 80/90/100 kV- and 140/150 kV-data sets as well as a weighted average image data set are derived. These merged data combine the advantages of increased (iodine) contrast at low energy level (80–90–100 kV) with the low noise at high energy level (140–150 kV), and could thus improve the contrast resolution for the detection of myocardial perfusion defects (16,34) (*Figure 4*).

Different vendors have re-introduced DECT and in recent years the technique has become clinically feasible. The DECT acquisition may be performed using a DSCT with two tubes simultaneously emitting higher (140–150 kV) and lower (80–90–100 kV) energy levels (35-37). A second approach consists of a single-source CT scanner with rapid kV switching (from 80 to 140 kV) to acquire the dual-energy samples almost simultaneously either in a single gantry rotation (GSI Cardiac; GE Healthcare), or in consecutive rotations (Acquilion One; Toshiba) (12,16,34). A third method involves a single X-ray source CT scanner operating at constant tube voltage with a sandwich detector technology in which the two detectors are superimposed and are composed of different materials (IQon Spectral CT, Philips Medical Systems) (12,16,34).

DECT perfusion allows for a quantitative analysis of the per-voxel amount of iodine concentration within the myocardium, expressed in mg/mL. Dual-energy derived color-coded iodine maps superimposed on the virtual non-contrast CT data allow the visualization of myocardial iodine distribution during the first pass, arterial phase, which might be considered as a surrogate marker of myocardial perfusion (*Figure 4*) (12,16,34).

Dynamic CTP imaging

In contrast to static CTP imaging, dynamic CTP imaging allows for acquisition of multiple phases before and during the first pass of a contrast bolus that enables the construction of the TACs of a reference artery and the myocardium.

There are two main different techniques in order to acquire a dynamic, time-resolved data sets: by using the DSCT scanner with the shuttle mode at two alternating table position enabling a coverage of 73 or 105 mm, respectively

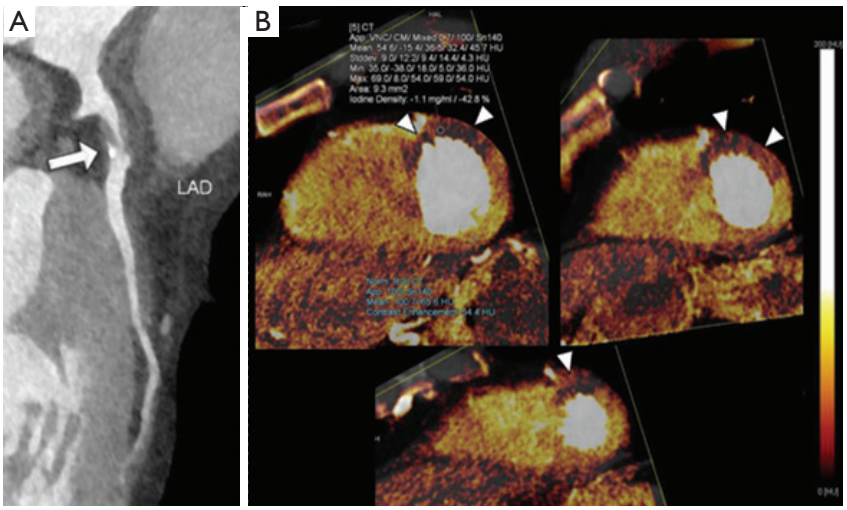

Figure 4 Static retrospectively ECG gated first pass dual-energy myocardial perfusion imaging. A 58-year-old male patient with history of atypical chest pain. (A) Coronary CT angiography showed a critical stenosis (>70% luminal narrowing) at the proximal segment of the left anterior descending artery (LAD) sustained by a mixed atherosclerotic plaque (arrow); (B) myocardial short-axis color-coded iodine distribution maps of dual-energy CT imaging during stress from basal to apical segments, show perfusion defects at the anteroseptal, anterior, and anterolateral wall corresponding to the territory of the LAD (arrowheads). Quantitative analysis of the dual-energy map at the level of the anterior wall shows a 42.8% reduction in iodine content (Iodine density: –1.1 mg/mL) with respect to the remote myocardium at the inferior wall.

for the second and third generation DSCT scanners; or by using a single-source 256- or 320-slice CT scanner with a wider detector Z-coverage of 78 or 160 mm, respectively, while the table is stationary (12,16). For both methods the acquisition lasts approximately 30 seconds during breath-hold and images are acquired during the late systole when the left ventricular myocardium is transmurally thicker and is shorter along the long axis, providing a more robust set for perfusion analysis. Furthermore end-systole is a shorter quiescent period compared to mid-diastole but is less sensitive to R-R variability and arrhythmia (12). Usually the amount of contrast medium administered is approximately 50 mL followed by 50 mL of saline at 5–6 mL/s.

Both semi-quantitative and fully quantitative perfusion methods are available for the dynamic CTP analysis. In a way similar for stress MRI perfusion, the semi-quantitative method evaluates the upslope of the TAC (upslope, time-to-peak, peak enhancement, and the area under the curve), and therefore it requires a lesser temporal sampling with the advantage of lower radiation dose (16). In contrast, the fully quantitative dynamic CTP imaging requires the complete wash-in and wash-out kinetics of contrast media and allows the quantification of MBF and volume and other hemodynamic parameters through the mathematical elaboration of TAC (16). In this case, the most common methods are deconvolution methods and its derivatives. By using the DSCT scanner, a modified parametric deconvolution technique based on a two-compartment model of intra- and extra-vascular space to fit the TAC is used (12,16). Using commercially available software (Volume Perfusion CT Body, Siemens), a double sampling of the arterial input function (AIF) to compensate for the shuttle mode is performed. The arterial TAC as well as the mean tissue time-attenuation curve is also derived automatically. Finally, mathematical elaboration of the TAC enables to calculate the MBF and the myocardial blood volume (MBV) of each myocardial voxel, generating a 3D color-coded parametric map, *Figure 5*. MBF expressed in mL/100 mL/min and MBV expressed in mL/100 mL are computed according to the formulas: MBF = MaxSlope(TissueTAC)/Maximum(AIF); MBV = Maximum(TissueTAC)/Maximum(AIF).

Semi-automated three-dimensional software has been developed for quantitative perfusion analysis with substantially reduced processing times, which is a beneficial step for integration dynamic CTP in a clinical

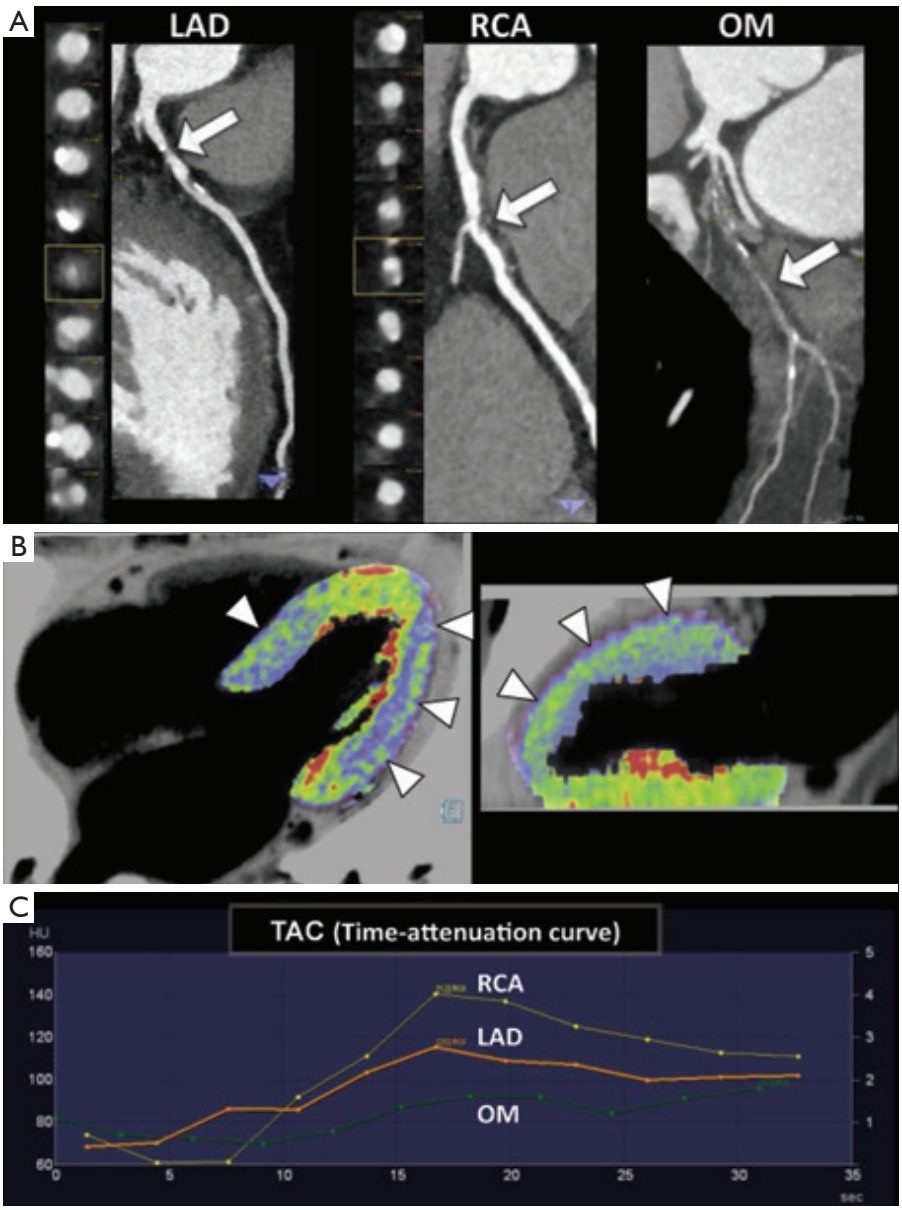

Figure 5 Dynamic CT myocardial perfusion imaging. A 60-year-old male patient with multiple cardiovascular risk factors presented with atypical chest pain. (A) Coronary CT angiography showed a critical stenosis (>70% luminal narrowing) at the proximal segment of the left anterior descending artery (LAD) and an intermediate stenosis at the middle segment of the right coronary artery (RCA) sustained by atherosclerotic plaques, arrows. Chronic total occlusion of the main obtuse marginal branch (OM) was documented too, arrow; (B) three-dimensional color-coded oblique 4-chamber (left) and 2-chamber (right) CT perfusion map images at stress show perfusion defects in the territory of the LAD (basal-middle septal wall and all segments of the anterior wall) and in the territory of the OM (lateral wall), color-coded in blue, arrowheads. The colors of the myocardium are coded according to the flow values with red, green, and yellow representing higher flow values than blue; (C) the corresponding tissue time-attenuation curves (TACs) of the myocardium from several consecutive acquisitions throughout the cardiac cycle at the inferior (yellow line), anterior (orange line), and lateral (green line) wall. Note the kinetics of the wash-in and wash-out of contrast media of the moderately ischemic myocardium (orange line) and severely ischemic myocardium (green line), with decreased wash-in and a reduced peak enhancement of the TACs, especially of the myocardial region supplied by the chronically occluded OM. The corresponding value of the hemodynamic parameters derived from the TACs, demonstrates a significant reduction of myocardial blood flow in the territory of the left coronary artery, especially in OM territory, consistent with inducible ischemia. Myocardial blood flow was 116.6 mL/100 mL/min, 81.6 mL/100 mL/min, and 45.3 mL/100 mL/min for the RCA, LAD and OM territories, respectively.

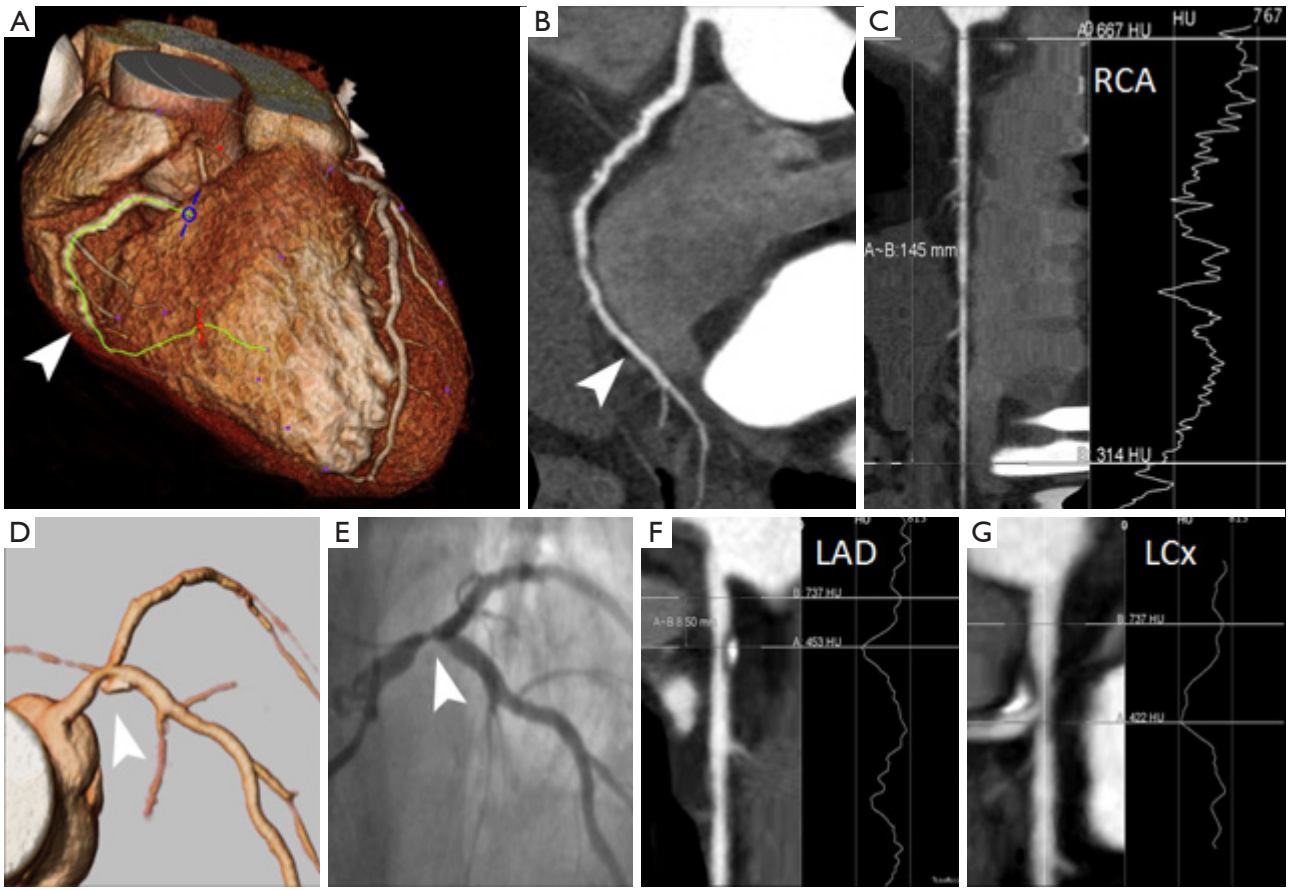

Figure 6 Transluminal Attenuation Gradient and Coronary Opacification. (A-C) Transluminal attenuation gradient (TAG) of an entire right coronary artery (A,B; arrowheads) with multiple intermediate lesions. The attenuation plot in C shows a progressive and irregular reduction of intraluminal attenuation from the proximal to the distal coronary artery; (D-G) coronary opacification (CO) difference across a severe stenosis (D-E; arrowheads) of the distal left main trunk involving the ostial left anterior descending (LAD; F) and left circumflex (LCx; G) arteries. RCA, right coronary artery; LAD, left anterior descending coronary artery; LCx, left circumflex coronary artery.

workflow (38).

Coronary flow/perfusion imaging and assessment

CT-derived fractional flow reserve (FFR-CT)

The FFR-CT method allows the extraction of 'stress induced' quantitative functional information from an anatomic CTA of at least moderate quality acquired at rest without adenosine infusion. The method uses computational fluid dynamics with simulated hyperemia to calculate the FFR measurement at any point in the vascular tree (39). The concept of coronary FFR, defined as the ratio of the mean coronary pressure distal to a coronary stenosis to the mean aortic pressure during maximal coronary blood flow, has evolved into an accepted functional measure of stenosis severity since first proposed 15 years ago (22). FFR has now become the invasive gold standard for assessing lesion-specific ischemia. A FFR value less than 0.80 or less than 0.75 identifies hemodynamic significance of coronary stenosis (7,8). FFR-CT correlates well with invasive-derived FFR measurements in patients with suspected or known CAD (17,39,40). One of the temporary drawbacks is that FFR-CT needs extreme computational ability and analysis time, which hampers widespread dissemination.

TAG

Coronary opacification (CO) and TAG are potential post-processing methods for noninvasive determination of lesion-specific ischemia by coronary CTA (*Figure 6*). Such as for FFR-CT, analysis of the intracoronary luminal

attenuation is available from standard coronary CTA data without modification of acquisition protocols or additional imaging, and has been known to reflect the intracoronary blood flow (41,42).

The method of CO refers to contrast attenuation difference across a stenosis, and was demonstrated to predict abnormal resting coronary blood flow (42).

However, the measurement of gradients across coronary stenosis is inherently more robust than evaluation of opacification difference. TAG is calculated as the slope of the linear regression produced by the luminal contrast attenuation (HU) from the ostium to the distal coronary vessel (43).

Two major drawbacks of the TAG method are the lack of temporal uniformity of the vessel attenuation when CTA data set relied on a multiple heartbeat acquisition, and severe coronary calcifications that may hamper accurate quantification. Therefore, two correction models have been proposed: the Corrected Coronary Opacification (TAG-CCO) on the same axial slice (the difference in attenuation values of coronary lumen measured before and after stenosis and normalized to the descending aorta), and the TAG with exclusion of calcified coronary segments (TAG-ExC) (44).

Results

CTP imaging

Several single center studies and the first multicenter trials have established the value of myocardial CTP imaging compared to reference standards as SPECT, ICA (with or without FFR) and stress perfusion MRI (*Tables 1-3*).

Myocardial CTP imaging appears clinically very attractive and able to improve diagnostic accuracy of coronary CTA, especially in terms of specificity and positive predictive value. A recent meta-analysis by Takx *et al.* including overall 37 studies (2,048 patients), evaluating the diagnostic accuracy of all commonly used myocardial perfusion imaging techniques with ICA and FFR as a reference standard for the diagnosis of hemodynamically significant CAD, have demonstrated that the performance of CTP imaging was comparable to that of stress MRI and PET, and superior to that of SPECT and echocardiography, with an overall sensitivity of 88% and specificity of 80% (64). Interestingly, CTP due to lesser false negative findings showed a higher sensitivity respect to SPECT (88% *vs.* 74%, respectively) (64). Accordingly, a prospective multicenter international trial, the CORE 320 study (n=381), has demonstrated that static CTP imaging has a superior diagnostic accuracy respect to SPECT in detecting obstructive coronary stenosis (≥50%) as compared with ICA (47). The higher sensitivity of CTP imaging was driven in part by its higher sensitivity in the detection of left main and multivessel CAD (47). The difference in diagnostic accuracy may be attributable to the superior spatial resolution of CTP respect to SPECT in the order of submillimeter, which allows detection of subtler subendocardial perfusion defects (47). Another explanation may be the more favorable extraction characteristics of the iodinated contrast material respect to Technetium-based tracers that are susceptible to the roll-off phenomenon, allowing for a linear relationship between CT-derived metrics and MBF (47).

Furthermore, the CORE 320 studies have shown that myocardial CTP analysis substantially increased the specificity and overall accuracy of coronary CTA to identify flow-limiting stenosis (CAD ≥50%) as determined by ICA and SPECT (48,50). This finding was true among patients with and without previous CAD, on both a per-patient and per-vessel level (48,50).

A recent randomized, multicenter, multivendor CTP study with regadenoson (n=110) by Cury *et al.*, has shown that CTP displayed a high sensitivity and specificity of 90% and 84%, respectively, for the detection of myocardial ischemia as defined by a reversible perfusion defect on SPECT (51). Similarly to the CORE 320 trials, regadenoson-CTP imaging improved the diagnostic accuracy of coronary CTA from 69% to 85%, which was primarily driven by a reduction in the rate of false positive CTA scans (51).

Furthermore, stress CTP has been proved to increase the diagnostic accuracy of coronary CTA also in patients with known CAD or high-risk profile, such as patients with implanted coronary stent or patients with heavy calcifications of the coronary tree (65-67).

Pooled results of another recent meta-analysis including 22 articles (1,507 subjects) showed acceptable diagnostic performance for all myocardial perfusion CT techniques (static as well as dynamic) compared to reference standards, including ICA, SPECT, and MRI, with sensitivity ranging from 75% to 89%, and specificity from 78% to 95% (68). It has emerged that static dual-energy and dynamic CTP imaging are associated with a trend towards higher sensitivity than standard static monoenergetic CTP (27). This may be related to the improved identification of subtle perfusion defects, which are easier to appreciate with the

Table 1 Static monoenergetic CT perfusion imaging studies

Author	N.	CT Technology	Analysis	Reference standard	SE (%)	SP (%)	PPV (%)	NPV (%)	Dose (mSv)
Blankstein *et al.*, 2009 (28)	34	First DSCT	Visual	SPECT (for vessel)	84	80	71	90	9.1
Rocha-Filho *et al.*, 2010 (29)	35	First DSCT	Visual	QCA (for vessel)	91	91	86	93	9.8
Feuchtner *et al.*, 2010 (32)	30	Second DSCT	Visual	MRI 1.5 T (for vessel)	96	88	93	94	0.93
Ko *et al.*, 2012 (45)	40	320-detector CT	TPR	FFR (for vessel)	74	66	56	81	4.5
			Visual[§]	FFR (for vessel)	87	95	89	94	
George *et al.*, 2012 (30)	50	320-detector CT	TPR	SPECT (for patient)	72	91	81	85	7.0
Bettencourt *et al.*, 2013 (46)	101	64-detector CT	Visual[§]	FFR (for patient)	89	83	80	90	5.0*
				MRI 1.5 T (for patient)	67	95	91	78	
Nasis *et al.*, 2013 (31)	20	320-detector CT	Visual[§]	QCA + SPECT (for patient)	94	98	94	98	4.8
George *et al.* (CORE320 study), 2014 (47)	381	320-detector CT	Semiq	QCA (for patient)	88	55	75	75	NA
Rochitte *et al.* (CORE320 study), 2014 (48)	381	320-detector CT	Semiq	QCA + SPECT (for patient)	80	74	65	86	5.31
Wong *et al.*, 2014 (49)	75	320-detector CT	Visual + TAG[§]	FFR (for vessel)	97	84	76	98	4.8
Magalhães *et al.* (CORE320 study), 2015 (50)	381	320-detector CT	Visual[§]	QCA + SPECT (for patient)	78	73	64	85	NA
Cury *et al.* (Regadenoson crossover study), 2015 (51)	110	Multivendor	Semiq	SPECT	90	82	53	97	17.7*
Yang *et al.*, 2015 (52)	75	Second DSCT	Visual	FFR (for patient)	89	86	96	63	6.5
				FFR (for vessel)	80	95	92	87	

All the studies but one (51) used adenosine at a dose of 0.14 mg/kg/min. Cury *et al*. used regadenoson at a dose of 0.4 mg (51). CT, computed tomography; DSCT, dual-source CT scanner; FFR, fractional flow reserve; mSv: millisievert; MRI, magnetic resonance imaging; N., number of patients; NA, non assessable; NPV, negative predictive value; PPV, positive predictive value; QCA, quantitative coronary angiography; SE, sensitivity; SP, specificity; Semiq, semiquantitative analysis using a stress score; SPECT, myocardial perfusion scan; TPR, transmural perfusion ratio; TAG, transluminal attenuation gradient. *, global radiation dose of the stress-rest protocol; [§], accuracy of CT perfusion integrated with the coronary anatomic data.

Table 2 Static dual-energy CT perfusion imaging studies

Author	N.	CT technology	Analysis	Reference standard	SE (%)	SP (%)	PPV (%)	NPV (%)	Dose (mSv)
Ko *et al.*, 2012 (35)	45	First DSCT	Iodine Map (for vessel)	QCA	89	74	80	85	5.7
Delgado *et al.*, 2013 (36)	56	Second DSCT	Iodine Map (for segment)	MRI 1.5T	76	99	89	98	5.2
Meinel *et al.*, 2014 (37)	55	Second DSCT	Iodine Map (for segment)	SPECT	99	97	92	100	7.1
Kido *et al.*, 2014 (53)	21	First/Second DSCT	Iodine Map (for vessel)[§]	QCA	67	92	84	82	7.7
Ko *et al.*, 2014 (54)	40	First DSCT	Iodine Map (for vessel)	QCA + MRI 3T[§]	87	79	71	91	4.6
Ko *et al.*, 2014 (55)	100	First DSCT	Iodine Map (for vessel)	QCA + MRI 1.5T and 3T[§]	88	79	73	91	4.2
Kim *et al.*, 2014 (56)	50	Second DSCT	Iodine Map (for segment)	MRI 1.5T	77	94	53	98	6.5

All the studies used adenosine at a dose of 0.14 mg/kg/min. Meinel *et al.* (37) used also a single injection of regadenoson at a dose of 0.4 mg. CT, computed tomography; DSCT, dual-source CT scanner; N., number of patients; mSv, millisievert; MRI, magnetic resonance imaging; NPV, negative predictive value; PPV, positive predictive value; QCA, quantitative coronary angiography; SE, sensitivity; SP, specificity; SPECT, myocardial perfusion scan. [§], accuracy of CT perfusion integrated with the coronary anatomic data.

Table 3 Dynamic CT perfusion imaging in human studies

Author, year	N.	CT technology	Reference standard	Analysis	SE (%)	SP (%)	PPV (%)	NPV (%)	Dose (mSv)
Ho *et al.*, 2010 (57)	35	Second DSCT	SPECT (segment)	Quantitative MBF	83	78	79	82	9.1
Bamberg *et al.*, 2011 (58)	33	Second DSCT	FFR[§] (vessel)	Quantitative MBF	93	87	75	97	10
Wang *et al.*, 2012 (59)	30	Second DSCT	QCA + SPECT (vessel)	Visual quantitative MBF and MBV	100	76	54	100	9.5
Huber *et al.*, 2013 (60)	32	256-detector CT	FFR (vessel)	Quantitative MBF	76	100	100	91	9.5
Greif *et al.*, 2013 (61)	65	Second DSCT	FFR (vessel)	Quantitative MBF	95	74	49	98	9.7
Rossi *et al.*, 2014 (62)	80	Second DSCT	FFR (vessel)	Quantitative MBF	88	90	77	95	9.4
Bamberg *et al.*, 2014 (63)	31	Second DSCT	MRI 3T (vessel)	Quantitative MBF and MBV	100	75	92	100	11.08

All the studies but one (57) used adenosine at a dose of 0.14 mg/kg/min. Ho et al. used dipyridamole at a dose of 0.56 mg/Kg (57). CT, computed tomography; DSCT, dual-source CT scanner; FFR, fractional flow reserve; N., number of patients; mSv, millisievert; MRI, magnetic resonance imaging; MBF, myocardial blood flow; MBV, myocardial blood volume; NPV, negative predictive value; PPV, positive predictive value; QCA, quantitative coronary angiography; SE, sensitivity; Semiq, semiquantitative analysis; SP, specificity; SPECT, myocardial perfusion scan. [§], accuracy of CT perfusion integrated with the coronary anatomic data.

Table 4 Dynamic CT perfusion imaging in animal studies

Author	N.	CT technology	Reference standard	Analysis	Dose (mSv)
Bamberg *et al.*, 2012 (70)	7 pigs	DS 2° g	Microsphere MBF	Quantitative MBF	10.6
Schwarz *et al.*, 2013 (71)	6 pigs	DS 2° g	Microsphere MBF	Quantitative MBF + attenuation values (HU)	11.3+0.88
Rossi *et al.*, 2013 (72)	7 pigs	DS 2° g	CBF and FFR	Quantitative MBF	17.1
Bamberg *et al.*, 2014 (73)	12 pigs	DS 2° g	Histopathology microsphere MBF	Quantitative MBF, MBV, K_{trans}	NA

All the studies but one (72) used adenosine at a dose of 0.14 mg/kg/min. Rossi *et al*. used adenosine at a dose of 0.50 mg/kg/min (72). CBF, coronary blood flow; CT, computed tomography; DSCT, dual-source CT scanner; FFR, fractional flow reserve; HU, Hounsfield unit; K_{trans}, permeability constant; mSv, millisievert; MBF, myocardial blood flow; MBV, myocardial blood volume; N., animals' number; NA, non assessable.

quantitative approaches (27).

In a recent study, Meinel *et al.* have demonstrated that a rest-stress CTP protocol should be the protocol of choice for dual-energy CTP imaging (37), with a sensitivity of 99%, specificity of 97%, positive predictive value (PPV) of 92% and NPV of 100% using SPECT as reference of standard. The addition of delayed enhancement didn't increase diagnostic accuracy, which therefore may be omitted reducing patient radiation exposure (37). An ongoing prospective, multicenter study, the DECIDE-Gold, will provide important evidence with regard to the accuracy of dual-energy CTP imaging for the depiction of lesion-specific ischemia (69).

Over the last five years, the feasibility of dynamic CTP imaging for absolute MBF quantification has been validated in experimental animal models demonstrating good correlation with fluorescent microsphere-derived MBF, histopathology and invasive measurements of coronary blood flow and FFR (*Table 4*). Interestingly, a recent large animal study have demonstrated that dynamic CTP has a superior discriminatory power in detecting myocardial ischemia than static first-pass CTP using fluorescent microspheres as a reference standard for MBF (71). In particular, dynamic CTP showed a notable difference in accuracy at lower degree of stenosis (50%), indicating that dynamic CTP may be more sensitive for the detection of subtle differences of myocardial perfusion as compared with single phase acquisitions (71).

In humans, quantitative dynamic CTP has shown to improve the overall diagnostic accuracy of coronary CTA in term of specificity and PPV (62,63), especially for interpretation of intermediate coronary lesions (30–70% luminal stenosis) compared with the reference standard of FFR (62).

In a recent multicenter clinical study on 146 patients, Meinel *et al.* (74) also demonstrated the utility of dynamic CT myocardial perfusion in the global quantitative assessment of left ventricular perfusion that can be particularly useful in the evaluation of patients with multivessel CAD and balanced ischemia. A cut-off value of 92 mL/100 mL/min has been proposed to distinguish between global myocardial hypoperfusion in the presence of three-vessel disease (74). However, different ischemic cut-off values of stress dynamic CTP to detect functionally significant coronary lesions have been proposed, ranging from 75 mL/100 mL/min to 103.1 mL/100 mL/min by using a DSCT scanner with invasive FFR measurement as the reference standard (16,27), and as high as 164 mL/100mL/min by using a 256-slices CT scanner (16). This wide range of cut-off values may be probably attributable to differences in study protocol, patient risk profile, prevalence of CAD, CT scanner technology and mathematical algorithms (16,60).

Furthermore, it is well known that MBF is related to numerous factors, such as age, gender, race, BMI, presence and severity of atherosclerosis, individual adaptive vasodilator response of the coronary arteriolar vessels and/or the presence of collateral flow (16,60).

Furthermore, considerable regional heterogeneity of the myocardial perfusion across coronary territories has been demonstrated in healthy and low-risk subjects (75,76). The natural intra-individual heterogeneity of regional MBF and large inter-individual range of MBF values have been previously documented in the PET and MRI literature (76), and necessitate the implementation of large databases on normal perfusion values such as for nuclear imaging to enable accurate interpretation of quantitative CTP data (27).

Finally, semi-quantitative parameters such as the TPR

Table 5 FFR-CT and TAG studies

Author, year	N.	SE (%)	SP (%)	PPV (%)	NPV (%)
FFR-CT studies					
DeFACTO, 2012 (40)	252	90	52	67	84
DISCOVER-FLOW, 2011 (17)	103	93	82	85	91
NXT, 2014 (79)	251	86	79	65	93
TAG studies					
Choi *et al.*, 2011 (43)	126	83	94	96	75
Wong *et al.*, 2013 (80)	54	77	74	67	86
Wong *et al.*, 2014 (49)	75	73	97	92	87
CTA + TAG + CTP	–	88	83	74	93
Stuijfzand *et al.*, 2014 (44)	85				
TAG	–	95	76	98	54
TAG-ExC	–	95	77	98	56
TAG-CCO	–	95	76	98	54

CCO, corrected coronary opacification; CT, computed tomography; CTA, CT angiography; N., number of patients; CTP, CT perfusion; FFR, fractional flow reserve; DeFACTO, Determination of Fractional Flow Reserve by Anatomic Computed Tomographic Angiography; DISCOVER-FLOW, Diagnosis of Ischemia-causing Stenoses Obtained Via Noninvasive Fractional Flow Reserve; NXT, Analysis of Coronary Blood Flow Using CT Angiography: Next Steps; TAG, transluminal attenuation gradient; TAG-ExC, TAG excluding calcified coronary segments; NPV, negative predictive value; PPV, positive predictive value; SE, sensitivity; SP, specificity.

and myocardial reserve index (difference in attenuation between the stress and rest phases) have been proposed for static myocardial CTP, however, they have demonstrated lower diagnostic accuracy than standard visual qualitative analysis (16,45,50). Similarly, a recent study by dynamic CTP showed that the TPR was inferior to quantified MBF with limited incremental value (77).

Finally, it is clearly important to establish the prognostic utility of CTP imaging beyond its diagnostic capabilities since myocardial perfusion imaging is widely used for risk stratification in clinical practice. A recent observational sub-study of the CATCH-trial has investigated the ability of adenosine static stress CTP scan performed in addition to conventional diagnostic evaluation to predict mid-term major adverse cardiac in patients with low-risk unstable angina pectoris (normal ECG and troponins). The study demonstrated a safe prognosis in patients referred for evaluation of acute onset chest pains with normal CTP; interestingly, the myocardial CTP pattern predicted mid-term clinical outcome, independently of the pretest probability of obstructive CAD. In particular, the worst prognosis was observed among patients with an extent of ischemic burden >10% of the left ventricular myocardium (78).

FFR-CT

Compared with morphologic CTA evaluation alone, the combination of CTA and FFR-CT provides improved diagnostic accuracy for the diagnosis of hemodynamically significant CAD, *Table 5*. Three prospective clinical trials by comparing FFR-CT with invasive FFR measurements in a binary fashion using a cut-off point of FFR ≤0.80 for lesion-specific ischemia, have demonstrated that FFR-CT improved diagnostic accuracy predominantly in terms of specificity and positive predictive value for detecting flow-obstructive vessel disease when used as a complement to CTA (17,40,79). In the DISCOVER-FLOW trial a significant correlation between FFR-CT and FFR values for per patient and per vessel analysis was demonstrated and both FFR-CT and FFR were not well correlated to percent diameter stenosis by quantitative ICA (17). Interestingly, a sub-analysis of the DISCOVER-FLOW trial has shown that FFR-CT significantly increased the accuracy of CTA

in evaluation of intermediate coronary stenosis as assessed by ICA (40–69%) (81). Similar results were confirmed by the multicenter DEFACTO trial that demonstrated a significant improvement of FFR-CT in the evaluation of intermediate severity lesions (30–70%) (40). Interestingly, the NXT trial demonstrated that FFR-CT was also superior in diagnostic accuracy for lesion specific ischemia compared to ICA lesion >50% (79).

A novel in-house CT-FFR prototype algorithm was used to expand CT-FFR utilization that increases its applicability in clinical practice, demonstrating good diagnostic CT-FFR performance similar to previously studies (82).

Another application of FFR-CT technology is the "virtual stenting" modeling that by predicting hemodynamic consequences after coronary stenting may be helpful in determining optimal revascularization strategies before invasive procedures (83).

Finally, a study evaluating the cost effectiveness of FFR-CT using data from the DISCOVER-FLOW trial suggests that FFR-CT is a cost-saving strategy with a 30% reduction of cost respect to ICA, principally due to deferred revascularizations (84).

TAG

The validity of TAG measurements compared to invasive FFR, as well as FFR-CT, has been evaluated extensively. It has been reported that TAG has the potential to improve the classification of stenosis severity on coronary CTA compared with ICA and FFR as a reference standard, especially in calcified lesions, which is particularly useful because heavy coronary calcification is a known drawback for CTA interpretation (43,80). However, wide variation in accuracy for detecting flow-obstructive vessel disease has been demonstrated (*Table 5*).

Wong *et al.* by using a 320-detector-row CT which enables near isophasic, single-beat imaging of the entire coronary tree, found that TAG provides acceptable prediction of invasive FFR and improved the accuracy of CTA for detecting significant stenosis (80). Conversely, Stuijfzand *et al.* showed that TAG and TAG-ExC, compared with FFR, failed to provide incremental diagnostic value over CTA in assessing lesion-specific ischemia. Only CCO was significantly lower in vessels with a hemodynamically significant lesion, but it was not possible to discriminate significant stenosis from low-grade stenosis (44).

Another application of the intracoronary attenuation-based analysis of the TAG has been tested in patients with totally occluded coronary arteries and could reflect the functional extent and direction (anterograde *vs.* retrograde) of coronary collateral flow (85).

Considerations on radiation dose

With the implementation of state of the art scanner the CTA and static perfusion study can be performed with low radiation dose. The introduction of tube current modulation, automatic tube potential and iterative reconstruction selection as well as prospective ECG-gating and high-pitch acquisition offer the ability to decrease dose below 3 mSv, often to sub-millisievert dose levels (32,33).

However, radiation exposure of dynamic CTP protocols remains a concern, although it is comparable with nuclear perfusion imaging studies (16,27). According to literature, an average value of 5.93 and 9.23 mSv for static and dynamic CTP has been reported, respectively (27). However, use of low tube voltage (80 kV) for the dynamic time-resolved acquisition may result in 40% dose reduction without affecting image quality and MBF quantification (86). Additionally, a tube current modulation technique and half-scan acquisition methods could substantially reduce radiation doses while maintaining diagnostic image quality (25). Furthermore, a statistical iterative reconstruction method implemented for dynamic CTP offers further potential for effective dose reduction (87).

Discussion

Advantages, limitations and future perspectives

The main limitations and strengths of different CT-based functional imaging techniques are summarized in *Table 6*.

While CTP seems sensitive and specific for evaluation of hemodynamically relevant CAD, studies so far are limited in size. Other limitations for the CTP imaging studies are the considerable variation in techniques and reference standards, and the heterogeneity of patient population.

An important limitation for static CTP is that it enables a qualitative evaluation of differences in contrast-enhancement between hypoperfused and normally perfused myocardium. Therefore, assessment of globally depressed myocardial perfusion in multi-vessel CAD may be undetected by static CTP imaging; however, balanced ischemia may be unmasked by identification of severe CAD on CT coronary angiography (27).

Noteworthy, the temporal resolution is crucial for

Table 6 Advantages and limitations of different CT-based functional imaging techniques

CT perfusion technique	Advantages	Limitations
Myocardial flow/perfusion imaging		
Static CTP imaging	Lower radiation exposure; rest-static CTP data set is derived from the coronary CTA acquisition; analysis of myocardial Iodine concentration with the dual-energy technique	No absolute quantification of MBF; globally reduced MBF in multivessel disease can be missed; state-of-the art technology required for dual-energy method; artifacts*
Dynamic CTP imaging	Absolute quantification of hemodynamic parameters (MBF and MBV); detection of diffuse ischemia in multivessel disease; assessment of absolute coronary flow reserve; evaluation of microvascular disease in symptomatic patients with or without nonobstructive CAD	Higher radiation exposure; state-of-the art technology; artifacts*; cannot be used for assessment of coronary anatomy
Coronary flow/perfusion imaging		
TAG/CO/COO	No additional CT scan is required; same radiation dose of coronary CTA; stress agent administration is not required	Indirect evaluation of FFR; lack of temporal uniformity of luminal attenuation values using a multiple heartbeat acquisitions; artifacts*
FFR-CT	Computation of a CT-derived FFR; no additional CT scan is required; same radiation dose of coronary CTA; stress agent administration is not required	Complex and prolonged post-processing computation by a remote supercomputer or on-site workstation; artifacts*

*, partial volume, beam hardening, motion, and breathing artifacts. CAD, coronary artery disease; CCO, corrected coronary opacification; CTA, computed tomography angiography; CTP, computed tomography perfusion; FFR, fractional flow reserve; MBF, myocardial blood flow; MBV, myocardial blood volume; TAG, transluminal attenuation gradient.

motion-free myocardial perfusion imaging. Newer CT technologies allows for more rapid data acquisition providing a temporal resolution as high as 66 ms with the third-generation dual source CT scanner (88). Moreover, the implementation of hybrid image reconstruction algorithm (89) preserves high temporal resolution of dual-source CT in dual-energy mode without affecting spectral separation.

Furthermore, several artifacts and pitfalls can affect CT-based functional imaging techniques and limit their clinical utility and accuracy.

Partial volume, beam hardening, motion, and breathing artifacts, may show false lower myocardial attenuation values incorrectly interpreted as perfusion defects and may in part explain the generally observed lower specificity and PPV.

In particular, motion artifacts due to increasing heart rate during stress myocardial CTP acquisition may be related to interpretability in a non-negligible percentage of patients (90).

The use of dual-energy CT due to its ability to generate virtual monochromatic images, may reduce the presence of beam hardening artifacts that can mimic the appearance of perfusion defects identified more frequently in the left ventricular posterobasal wall (16).

Challenges specific to dynamic CTP imaging, next to high radiation exposure from dynamic acquisition, include the beam hardening artifacts and the requirement for breath holding over 30 s that may lead to respiratory motion. However, beam hardening and motion correction algorithms are readily available and can minimize the effect of these artifacts.

The main strength of CT-based functional imaging techniques is the unique ability to offer a combined anatomic and functional evaluation of ischemic heart disease in the same examination. Only one images data set at rest is required for the FFR-CT or TAG method to assess both coronary anatomy and lesion-specific ischemia, whereas a stepwise approach at rest and during stress is necessary for the static and dynamic CTP imaging. Conversely, the commonly used hybrid SPECT-CT or PET-CT modalities require two separate imaging procedures, resulting in additional cost and radiation exposure. Therefore, CT-based functional imaging may be considered the unique stand-alone integrated hybrid imaging technique.

FFR-CT is the first noninvasive functional test to use an outcome-based gold standard, that is invasive FFR, rather than one fundamentally based on coronary stenosis measurement (39). The benefits clearly reside in the reduced false positives compared with CTA alone,

with the concomitant reduction in unnecessary ICA. However, major limitations are that a long and complex post-processing using dedicated off-site or in-house software and an adequate CTA image quality are required. Therefore, further data are needed on its clinical- and cost-effectiveness outside of clinical trials in the real-world experience. Recently, a new CT-based method termed transluminal attenuation flow encoding (TAFE) for noninvasive measurement of absolute coronary blood flow was validated in animal model and in a feasibility clinical study (91). TAFE allows for quantification of absolute CBF from a standard CT acquisition using contrast distribution, TAG, and AIF and correlates well with reference standard measurements of MBF in animals (91). TAFE may provide functional significance of CAD without complex computational methods and has the potential to be integrated in computational fluid dynamics modeling, significantly simplifying CT-based FFR calculations (91).

Furthermore, a machine-learning-based model for predicting FFR has been proposed as an alternative to physics-based approaches, with an excellent correlation of measured FFR and the advantage of consistent reduction of execution time (92).

Unlike FFR-CT, TAG depends on the luminal attenuation values and it does not require complex computation. However, accuracy of quantification may be influenced by various artifacts on CTA, therefore maintaining adequate image quality of CTA is crucial for TAG analysis. Given the limited evidence so far, larger studies with current acquisition and reconstruction protocols as well as new analysis software are required to validate the diagnostic and prognostic value of this approach.

Beyond the assessment of regional MBF quantification, another advantage of quantitative analysis of CTP over to the qualitative and semi-quantitative approaches is the ability to compute absolute coronary flow reserve (CFR), calculated as the ratio of MBF at stress to MBF at rest. Most of the existing evidences on global myocardial flow have utilized PET flow imaging, with values of rest and hyperemic flow ranging from 0.65 to 1.10 and 1.86 to 4.35 mL/g/min, and a CFR value of 3.16–4.99 (76). However, the rest and hyperemic flow in the CTP studies is within the documented range of that in PET studies, though the CFR is systematically lower due to an underestimation of MBF, with values in the range of 1.5–2.0 (76,93). Probably this difference may be related to intrinsic differences in the techniques and contrast or tracer uptake kinetics, to the two-compartment model analysis and limited temporal sampling of dynamic CTP.

Another future impact of quantitative dynamic CTP imaging in a way similar to PET imaging is the identification of an abnormally reduced hyperemic MBF in the absence of obstructive CAD in patients with microvascular dysfunction, but this potential application needs to be investigated in the near future.

The quantification of MBF also may proof helpful to identify the potential source of angina symptoms in patients with nonobstructive coronary disease, in the context of arterial hypertension and diabetes mellitus (94), or different phenotypes of hypertrophic cardiomyopathy.

Finally, validation and standardization of myocardial perfusion CT is essential for successful clinical implementation but it still ongoing.

Conclusions

CT-based functional imaging improves diagnostic accuracy of coronary CTA in both patients with suspected and known CAD.

A number of protocols for CTP imaging are available, which can assess myocardial perfusion in both a qualitative, semi-quantitative or quantitative manner. Probably, the optimum imaging technique will depend on the clinical question, local available technology and the individual patient characteristics (pre-test probability of CAD and CAD burden).

The interpretation of stress CTP images needs to be integrated also with the underlying coronary morphology (and wall motion analysis) to become a potential more effective gatekeeper for ICA with a better stratification of patients that would benefit from revascularization.

In this view, CT functional imaging has the unique advantage to provide a comprehensive anatomical and functional evaluation in a single examination. Ongoing developments of both hardware (spatial, temporal and contrast resolution, detector technology) and software (for a more reliable and robust integration in clinical practice) will substantially enhance the future impact of CT imaging in the clinical workflow of CAD patients.

However, further evaluation in large-scale clinical trials is warranted to assess the effective clinical role of CT functional imaging in terms of accuracy and costs in relation to other commonly used functional imaging techniques.

Ultimately, future prognostic studies will be required to show that combining CT-based functional imaging with coronary CTA not only improves diagnostic accuracy, but

may also lead to better patient management and outcomes.

Acknowledgements

None.

Footnote

Conflicts of Interest: The authors have no conflicts of interest to declare.

References

1. Mark DB, Berman DS, Budoff MJ, et al. ACCF/ACR/AHA/NASCI/SAIP/SCAI/SCCT 2010 expert consensus document on coronary computed tomographic angiography: a report of the American College of Cardiology Foundation Task Force on Expert Consensus Documents. Circulation 2010;121:2509-43.
2. Montalescot G, Sechtem U, Achenbach S, et al. 2013 ESC guidelines on the management of stable coronary artery disease: the Task Force on the management of stable coronary artery disease of the European Society of Cardiology. Eur Heart J 2013;34:2949-3003.
3. Munnur RK, Cameron JD, Ko BS, et al. Cardiac CT: atherosclerosis to acute coronary syndrome. Cardiovasc Diagn Ther 2014;4:430-48.
4. Yang L, Zhou T, Zhang R, et al. Meta-analysis: diagnostic accuracy of coronary CT angiography with prospective ECG gating based on step-and-shoot, Flash and volume modes for detection of coronary artery disease. Eur Radiol 2014;24:2345-52.
5. Min JK, Dunning A, Lin FY, et al. Age- and sex-related differences in all-cause mortality risk based on coronary computed tomography angiography findings results from the International Multicenter CONFIRM (Coronary CT Angiography Evaluation for Clinical Outcomes: An International Multicenter Registry) of 23,854 patients without known coronary artery disease. J Am Coll Cardiol 2011;58:849-60.
6. Andreini D, Pontone G, Mushtaq S, et al. A long-term prognostic value of coronary CT angiography in suspected coronary artery disease. JACC Cardiovasc Imaging 2012;5:690-701.
7. Tonino PA, Fearon WF, De Bruyne B, et al. Angiographic versus functional severity of coronary artery stenoses in the FAME study fractional flow reserve versus angiography in multivessel evaluation. J Am Coll Cardiol 2010;55:2816-21.
8. De Bruyne B, Pijls NH, Kalesan B, et al. Fractional flow reserve-guided PCI versus medical therapy in stable coronary disease. N Engl J Med 2012;367:991-1001.
9. Boden WE, O'Rourke RA, Teo KK, et al. Optimal medical therapy with or without PCI for stable coronary disease. N Engl J Med 2007;356:1503-16.
10. van Werkhoven JM, Schuijf JD, Gaemperli O, et al. Prognostic value of multislice computed tomography and gated single-photon emission computed tomography in patients with suspected coronary artery disease. J Am Coll Cardiol 2009;53:623-32.
11. Adams DF, Hessel SJ, Judy PF, et al. Computed tomography of the normal and infarcted myocardium. AJR Am J Roentgenol 1976;126:786-91.
12. Rossi A, Merkus D, Klotz E, et al. Stress myocardial perfusion: imaging with multidetector CT. Radiology 2014;270:25-46.
13. Kurata A, Mochizuki T, Koyama Y, et al. Myocardial perfusion imaging using adenosine triphosphate stress multi-slice spiral computed tomography: alternative to stress myocardial perfusion scintigraphy. Circ J 2005;69:550-7.
14. van Rosendael AR, de Graaf MA, Scholte AJ. Myocardial CT perfusion for the prediction of obstructive coronary artery disease, valuable or not? Cardiovasc Diagn Ther 2015;5:63-6.
15. Sun Z. Evidence for myocardial CT perfusion imaging in the diagnosis of hemodynamically significant coronary artery disease. Cardiovasc Diagn Ther 2015;5:58-62.
16. Seitun S, Castiglione Morelli M, Budaj I, et al. Stress computed tomography myocardial perfusion imaging: a new topic in cardiology. Rev Esp Cardiol (Engl Ed) 2016;69:188-200.
17. Koo BK, Erglis A, Doh JH, et al. Diagnosis of ischemia-causing coronary stenoses by noninvasive fractional flow reserve computed from coronary computed tomographic angiograms. Results from the prospective multicenter DISCOVER-FLOW (Diagnosis of Ischemia-Causing Stenoses Obtained Via Noninvasive Fractional Flow Reserve) study. J Am Coll Cardiol 2011;58:1989-97.
18. de Feyter PJ. CT functional imaging using intracoronary gradient analysis: an indispensable boost for CT coronary angiography. Eur Heart J Cardiovasc Imaging 2012;13:971-2.
19. Techasith T, Cury RC. Stress myocardial CT perfusion: an update and future perspective. JACC Cardiovasc Imaging 2011;4:905-16.

20. Mehra VC, Valdiviezo C, Arbab-Zadeh A, et al. A stepwise approach to the visual interpretation of CT-based myocardial perfusion. J Cardiovasc Comput Tomogr 2011;5:357-69.
21. Salerno M, Beller GA. Noninvasive assessment of myocardial perfusion. Circ Cardiovasc Imaging 2009;2:412-24.
22. Gould KL, Lipscomb K, Hamilton GW. Physiologic basis for assessing critical coronary stenosis. Instantaneous flow response and regional distribution during coronary hyperemia as measures of coronary flow reserve. Am J Cardiol 1974;33:87-94.
23. Cerqueira MD, Weissman NJ, Dilsizian V, et al. Standardized myocardial segmentation and nomenclature for tomographic imaging of the heart: a statement for healthcare professionals from the Cardiac Imaging Committee of the Council on Clinical Cardiology of the American Heart Association. Circulation 2002;105:539-42.
24. Bischoff B, Bamberg F, Marcus R, et al. Optimal timing for first-pass stress CT myocardial perfusion imaging. Int J Cardiovasc Imaging 2013;29:435-42.
25. Kim SM, Kim YN, Choe YH. Adenosine-stress dynamic myocardial perfusion imaging using 128-slice dual-source CT: optimization of the CT protocol to reduce the radiation dose. Int J Cardiovasc Imaging 2013;29:875-84.
26. Tanabe Y, Kido T, Kurata A, et al. Optimal Scan Time for Single-Phase Myocardial Computed Tomography Perfusion to Detect Myocardial Ischemia-Derivation Cohort From Dynamic Myocardial Computed Tomography Perfusion. Circ J 2016;80:2506-12.
27. Danad I, Szymonifka J, Schulman-Marcus J, et al. Static and dynamic assessment of myocardial perfusion by computed tomography. Eur Heart J Cardiovasc Imaging 2016;17:836-44.
28. Blankstein R, Shturman LD, Rogers IS, et al. Adenosine-induced stress myocardial perfusion imaging using dual-source cardiac computed tomography. J Am Coll Cardiol 2009;54:1072-84.
29. Rocha-Filho JA, Blankstein R, Shturman LD, et al. Incremental value of adenosine-induced stress myocardial perfusion imaging with dual-source CT at cardiac CT angiography. Radiology 2010;254:410-9.
30. George RT, Arbab-Zadeh A, Miller JM, et al. Computed tomography myocardial perfusion imaging with 320-row detector computed tomography accurately detects myocardial ischemia in patients with obstructive coronary artery disease. Circ Cardiovasc Imaging 2012;5:333-40.
31. Nasis A, Ko BS, Leung MC, et al. Diagnostic accuracy of combined coronary angiography and adenosine stress myocardial perfusion imaging using 320-detector computed tomography: pilot study. Eur Radiol 2013;23:1812-21.
32. Feuchtner G, Goetti R, Plass A, et al. Adenosine stress high-pitch 128-slice dual-source myocardial computed tomography perfusion for imaging of reversible myocardial ischemia: comparison with magnetic resonance imaging. Circ Cardiovasc Imaging 2011;4:540-9.
33. Maffei E, Martini C, De Crescenzo S, et al. Low dose CT of the heart: a quantum leap into a new era of cardiovascular imaging. Radiol Med 2010;115:1179-207.
34. Danad I, Ó Hartaigh B, Min JK. Dual-energy computed tomography for detection of coronary artery disease. Expert Rev Cardiovasc Ther 2015;13:1345-56.
35. Ko SM, Choi JW, Hwang HK, et al. Diagnostic performance of combined noninvasive anatomic and functional assessment with dual-source CT and adenosine-induced stress dual-energy CT for detection of significant coronary stenosis. AJR Am J Roentgenol 2012;198:512-20.
36. Delgado C, Vázquez M, Oca R, et al. Myocardial ischemia evaluation with dual-source computed tomography: comparison with magnetic resonance imaging. Rev Esp Cardiol (Engl Ed) 2013;66:864-70.
37. Meinel FG, De Cecco CN, Schoepf UJ, et al. First-arterial-pass dual-energy CT for assessment of myocardial blood supply: do we need rest, stress, and delayed acquisition? Comparison with SPECT. Radiology 2014;270:708-16.
38. Ebersberger U, Marcus RP, Schoepf UJ, et al. Dynamic CT myocardial perfusion imaging: performance of 3D semi-automated evaluation software. Eur Radiol 2014;24:191-9.
39. Hecht HS, Narula J, Fearon WF. Fractional flow reserve and coronary computed tomographic angiography: a review and critical analysis. Circ Res 2016;119:300-16.
40. Min JK, Leipsic J, Pencina MJ, et al. Diagnostic accuracy of fractional flow reserve from anatomic CT angiography. JAMA 2012;308:1237-45.
41. Steigner ML, Mitsouras D, Whitmore AG, et al. Iodinated contrast opacification gradients in normal coronary arteries imaged with prospectively ECG-gated single heart beat 320-detector row computed tomography. Circ Cardiovasc Imaging 2010;3:179-86.
42. Chow BJ, Kass M, Gagné O, et al. Can differences in corrected coronary opacification measured with computed tomography predict resting coronary artery flow? J Am Coll Cardiol 2011;57:1280-8.

43. Choi JH, Min JK, Labounty TM, et al. Intracoronary transluminal attenuation gradient in coronary CT angiography for determining coronary artery stenosis. JACC Cardiovasc Imaging 2011;4:1149-57.
44. Stuijfzand WJ, Danad I, Raijmakers PG, et al. Additional value of transluminal attenuation gradient in CT angiography to predict hemodynamic significance of coronary artery stenosis. JACC Cardiovasc Imaging 2014;7:374-86.
45. Ko BS, Cameron JD, Leung M, et al. Combined CT coronary angiography and stress myocardial perfusion imaging for hemodynamically significant stenoses in patients with suspected coronary artery disease: a comparison with fractional flow reserve. JACC Cardiovasc Imaging 2012;5:1097-111.
46. Bettencourt N, Ferreira ND, Leite D, et al. CAD detection in patients with intermediate-high pre-test probability: low-dose CT delayed enhancement detects ischemic myocardial scar with moderate accuracy but does not improve performance of a stress-rest CT perfusion protocol. JACC Cardiovasc Imaging 2013;6:1062-71.
47. George RT, Mehra VC, Chen MY, et al. Myocardial CT perfusion imaging and SPECT for the diagnosis of coronary artery disease: a head-to-head comparison from the CORE320 multicenter diagnostic performance study. Radiology 2014;272:407-16.
48. Rochitte CE, George RT, Chen MY, et al. Computed tomography angiography and perfusion to assess coronary artery stenosis causing perfusion defects by single photon emission computed tomography: the CORE320 study. Eur Heart J 2014;35:1120-30.
49. Wong DT, Ko BS, Cameron JD, et al. Comparison of diagnostic accuracy of combined assessment using adenosine stress computed tomography perfusion + computed tomography angiography with transluminal attenuation gradient + computed tomography angiography against invasive fractional flow reserve. J Am Coll Cardiol 2014;63:1904-12.
50. Magalhães TA, Kishi S, George RT, et al. Combined coronary angiography and myocardial perfusion by computed tomography in the identification of flow-limiting stenosis - The CORE320 study: An integrated analysis of CT coronary angiography and myocardial perfusion. J Cardiovasc Comput Tomogr 2015;9:438-45.
51. Cury RC, Kitt TM, Feaheny K, et al. A randomized, multicenter, multivendor study of myocardial perfusion imaging with regadenoson CT perfusion vs single photon emission CT. J Cardiovasc Comput Tomogr 2015;9:103-12.e1-2.
52. Yang DH, Kim YH, Roh JH, et al. Stress Myocardial perfusion CT in patients suspected of having coronary artery disease: visual and quantitative analysis-validation by using fractional flow reserve. Radiology 2015;276:715-23.
53. Kido T, Watanabe K, Saeki H, et al. Adenosine triphosphate stress dual-source computed tomography to identify myocardial ischemia: comparison with invasive coronary angiography. Springerplus 2014;3:75.
54. Ko SM, Park JH, Hwang HK, et al. Direct comparison of stress- and rest-dual-energy computed tomography for detection of myocardial perfusion defect. Int J Cardiovasc Imaging 2014;30 Suppl 1:41-53.
55. Ko SM, Song MG, Chee HK, et al. Diagnostic performance of dual-energy CT stress myocardial perfusion imaging: direct comparison with cardiovascular MRI. AJR Am J Roentgenol 2014;203:W605-13.
56. Kim SM, Chang SA, Shin W, et al. Dual-energy CT perfusion during pharmacologic stress for the assessment of myocardial perfusion defects using a second-generation dual-source CT: a comparison with cardiac magnetic resonance imaging. J Comput Assist Tomogr 2014;38:44-52.
57. Ho KT, Chua KC, Klotz E, et al. Stress and rest dynamic myocardial perfusion imaging by evaluation of complete time-attenuation curves with dual-source CT. JACC Cardiovasc Imaging 2010;3:811-20.
58. Bamberg F, Becker A, Schwarz F, et al. Detection of hemodynamically significant coronary artery stenosis: incremental diagnostic value of dynamic CT-based myocardial perfusion imaging. Radiology 2011;260:689-98.
59. Wang Y, Qin L, Shi X, et al. Adenosine-stress dynamic myocardial perfusion imaging with second-generation dual-source CT: comparison with conventional catheter coronary angiography and SPECT nuclear myocardial perfusion imaging. AJR Am J Roentgenol 2012;198:521-9.
60. Huber AM, Leber V, Gramer BM, et al. Myocardium: dynamic versus single-shot CT perfusion imaging. Radiology 2013;269:378-86.
61. Greif M, von Ziegler F, Bamberg F, et al. CT stress perfusion imaging for detection of haemodynamically relevant coronary stenosis as defined by FFR. Heart 2013;99:1004-11.
62. Rossi A, Dharampal A, Wragg A, et al. Diagnostic performance of hyperaemic myocardial blood flow index obtained by dynamic computed tomography: does it predict functionally significant coronary lesions? Eur Heart J Cardiovasc Imaging 2014;15:85-94.

63. Bamberg F, Marcus RP, Becker A, et al. Dynamic myocardial CT perfusion imaging for evaluation of myocardial ischemia as determined by MR imaging. JACC Cardiovasc Imaging 2014;7:267-77.
64. Takx RA, Blomberg BA, El Aidi H, et al. Diagnostic accuracy of stress myocardial perfusion imaging compared to invasive coronary angiography with fractional flow reserve meta-analysis. Circ Cardiovasc Imaging 2015;8(1).
65. Rief M, Zimmermann E, Stenzel F, et al. Computed tomography angiography and myocardial computed tomography perfusion in patients with coronary stents: prospective intraindividual comparison with conventional coronary angiography. J Am Coll Cardiol 2013;62:1476-85.
66. Sharma RK, Arbab-Zadeh A, Kishi S, et al. Incremental diagnostic accuracy of computed tomography myocardial perfusion imaging over coronary angiography stratified by pre-test probability of coronary artery disease and severity of coronary artery calcification: The CORE320 study. Int J Cardiol 2015;201:570-7.
67. Bischoff B, Deseive S, Rampp M, et al. Myocardial ischemia detection with single-phase CT perfusion in symptomatic patients using high-pitch helical image acquisition technique. Int J Cardiovasc Imaging 2017;33:569-76.
68. Pelgrim GJ, Dorrius M, Xie X, et al. The dream of a one-stop-shop: Meta-analysis on myocardial perfusion CT. Eur J Radiol 2015;84:2411-20.
69. Truong QA, Knaapen P, Pontone G, et al. Rationale and design of the dual-energy computed tomography for ischemia determination compared to "gold standard" noninvasive and invasive techniques (DECIDE-Gold): A multicenter international efficacy diagnostic study of rest-stress dual-energy computed tomography angiography with perfusion. J Nucl Cardiol 2015;22:1031-40.
70. Bamberg F, Hinkel R, Schwarz F, et al. Accuracy of dynamic computed tomography adenosine stress myocardial perfusion imaging in estimating myocardial blood flow at various degrees of coronary artery stenosis using a porcine animal model. Invest Radiol 2012;47:71-7.
71. Schwarz F, Hinkel R, Baloch E, et al. Myocardial CT perfusion imaging in a large animal model: comparison of dynamic versus single-phase acquisitions. JACC Cardiovasc Imaging 2013;6:1229-38.
72. Rossi A, Uitterdijk A, Dijkshoorn M, et al. Quantification of myocardial blood flow by adenosine-stress CT perfusion imaging in pigs during various degrees of stenosis correlates well with coronary artery blood flow and fractional flow reserve. Eur Heart J Cardiovasc Imaging 2013;14:331-8.
73. Bamberg F, Hinkel R, Marcus RP, et al. Feasibility of dynamic CT-based adenosine stress myocardial perfusion imaging to detect and differentiate ischemic and infarcted myocardium in an large experimental porcine animal model. Int J Cardiovasc Imaging 2014;30:803-12.
74. Meinel FG, Ebersberger U, Schoepf UJ, et al. Global quantification of left ventricular myocardial perfusion at dynamic CT: feasibility in a multicenter patient population. AJR Am J Roentgenol 2014;203:W174-80.
75. Kim EY, Chung WJ, Sung YM, et al. Normal range and regional heterogeneity of myocardial perfusion in healthy human myocardium: assessment on dynamic perfusion CT using 128-slice dual-source CT. Int J Cardiovasc Imaging 2014;30 Suppl 1:33-40.
76. Ho KT, Ong HY, Tan G, et al. Dynamic CT myocardial perfusion measurements of resting and hyperaemic blood flow in low-risk subjects with 128-slice dual-source CT. Eur Heart J Cardiovasc Imaging 2015;16:300-6.
77. Coenen A, Lubbers MM, Kurata A, et al. Diagnostic value of transmural perfusion ratio derived from dynamic CT-based myocardial perfusion imaging for the detection of haemodynamically relevant coronary artery stenosis. Eur Radiol 2016. [Epub ahead of print].
78. Linde JJ, Sørgaard M, Kühl JT, et al. Prediction of clinical outcome by myocardial CT perfusion in patients with low-risk unstable angina pectoris. Int J Cardiovasc Imaging 2017;33:261-70.
79. Nørgaard BL, Leipsic J, Gaur S, et al. Diagnostic performance of noninvasive fractional flow reserve derived from coronary computed tomography angiography in suspected coronary artery disease: the NXT trial (Analysis of Coronary Blood Flow Using CT Angiography: Next Steps). J Am Coll Cardiol 2014;63:1145-55.
80. Wong DT, Ko BS, Cameron JD, et al. Transluminal attenuation gradient in coronary computed tomography angiography is a novel noninvasive approach to the identification of functionally significant coronary artery stenosis: a comparison with fractional flow reserve. J Am Coll Cardiol 2013;61:1271-9.
81. Min JK, Koo BK, Erglis A, et al. Usefulness of noninvasive fractional flow reserve computed from coronary computed tomographic angiograms for intermediate stenoses confirmed by quantitative coronary angiography. Am J Cardiol 2012;110:971-6.
82. Baumann S, Wang R, Schoepf UJ, et al. Coronary CT angiography-derived fractional flow reserve correlated with invasive fractional flow reserve measurements--initial

experience with a novel physician-driven algorithm. Eur Radiol 2015;25:1201-7.
83. Kim KH, Doh JH, Koo BK, et al. A novel noninvasive technology for treatment planning using virtual coronary stenting and computed tomography-derived computed fractional flow reserve. JACC Cardiovasc Interv 2014;7:72-8.
84. Hlatky MA, Saxena A, Koo BK, et al. Projected costs and consequences of computed tomography-determined fractional flow reserve. Clin Cardiol 2013;36:743-8.
85. Choi JH, Kim EK, Kim SM, et al. Noninvasive evaluation of coronary collateral arterial flow by coronary computed tomographic angiography. Circ Cardiovasc Imaging 2014;7:482-90.
86. Fujita M, Kitagawa K, Ito T, et al. Dose reduction in dynamic CT stress myocardial perfusion imaging: comparison of 80-kV/370-mAs and 100-kV/300-mAs protocols. Eur Radiol 2014;24:748-55.
87. Tao Y, Chen GH, Hacker TA, et al. Low dose dynamic CT myocardial perfusion imaging using a statistical iterative reconstruction method. Medical Physics 2014;41:071914.
88. Morsbach F, Gordic S, Desbiolles L, et al. Performance of turbo high-pitch dual-source CT for coronary CT angiography: first ex vivo and patient experience. Eur Radiol 2014;24:1889-95.
89. Nance JW Jr, Bastarrika G, Kang DK, et al. High-temporal resolution dual-energy computed tomography of the heart using a novel hybrid image reconstruction algorithm: initial experience. J Comput Assist Tomogr 2011;35:119-25.
90. van Rosendael AR, de Graaf MA, Dimitriu-Leen AC, et al. The influence of clinical and acquisition parameters on the interpretability of adenosine stress myocardial computed tomography perfusion. Eur Heart J Cardiovasc Imaging 2017;18:203-11.
91. Lardo AC, Rahsepar AA, Seo JH, et al. Estimating coronary blood flow using CT transluminal attenuation flow encoding: Formulation, preclinical validation, and clinical feasibility. J Cardiovasc Comput Tomogr 2015;9:559-66.e1.
92. Itu L, Rapaka S, Passerini T, et al. A machine-learning approach for computation of fractional flow reserve from coronary computed tomography. J Appl Physiol (1985) 2016;121:42-52.
93. Marini C, Seitun S, Zawaideh C, et al. Comparison of coronary flow reserve estimated by dynamic radionuclide SPECT and multi-detector x-ray CT. J Nucl Cardiol 2016. [Epub ahead of print].
94. Vliegenthart R, De Cecco CN, Wichmann JL, et al. Dynamic CT myocardial perfusion imaging identifies early perfusion abnormalities in diabetes and hypertension: Insights from a multicenter registry. J Cardiovasc Comput Tomogr 2016;10:301-8.

Cite this article as: Cademartiri F, Seitun S, Clemente A, La Grutta L, Toia P, Runza G, Midiri M, Maffei E. Myocardial blood flow quantification for evaluation of coronary artery disease by computed tomography. Cardiovasc Diagn Ther 2017;7(2):129-150. doi: 10.21037/cdt.2017.03.22

